Chapter 7

Significantly enhanced coupling efficiency in 2D photonic crystal waveguides by using cabin-side-like tapered structures at two terminals

A paper was accepted by the Japanese Journal of Applied Physics Part2, Letter, 2004. Vol. 43, B08, in press

7.1 Introduction

With the development and implementation of integrated optical circuits (IOCs), telecommunication systems can now be made compact in size with low cost. In addition to addressing the technological challenges involved in realizing the integrated circuits, there are various critical problems that need to be solved to perfect the coupling between the conventional silica waveguide (SWG) and IOC. Because IOCs are compatible with standard planar semiconductor processing technology, and thus it is possible achieve the combination and integration of IOCs with active optoelectronic devices on a single chip, the planar photonic crystal waveguides (PPCWGs) have become the subject of active interest because of their potential applications in mini-telecommunication systems, in which complex IOCs are required.[1,2] Consequently, the integration of PPCGWs with active elements on a single chip is expected to provide a compact mode converter with a high transmission efficiency, and this will be a key building block for highly complex devices.

The achievement of the efficient coupling of light waves at the entrance and exit ports of the PPCWGs is a difficult task because conventional index waveguides and PPCWGs are based on differerent physical mechanisms and possess different width, for example, the width of PPCWGs is small, being approximatively on the order of 0.6μm for both SWG and W1(i.e., one row of dielectric rods along the Γ-K direction is removed) PPCWGs when they are realized in the IOCs. Thus, a considerable drawback is encountered when one attempts to efficiently. test novel PC devices. Strong reflection and scattering from the ends of the PCWG appear, which adversely reduce the transmitted probability measured. On the contrary, using tapered integrated waveguides can significantly improve the coupling of light waves, as reported in refs.[3,4] However, the utilization of this kind of structure is limited because the refractive index of the material surrounding the rods in the PPC waveguide should always be different from that of the IOC waveguide, and their method is only useful if light is strongly confined in the waveguide.

Recently, the improved coupling structure in the PPCWGs was designed and experimentally verified in refs.[5,6] by gradually varying the rod size at the ends of the PPCWGs. Furthermore, a coupling technique based on employing four in-axis (in the W1 direction) circular defect rods[7] and twelve off-axis (not in the W1 direction) elliptical Si defect rods[8] by adjusting the radii and positions of defects within the conventional PPCWG tapers has been reported. Although a high peak transmission of up to 80% was achieved over a certain finite range of frequencies, however, it still is difficult to design the optical tapered structural configuration and control the rod sizes with the required accuracy in practical fabrication.

7.2 Structure and coupling techniques

Motivated by these previous works and addressing the challenges, in this chapter, we propose and design cabin-side-like tapered structures which are placed at the entrance and exit terminals of the PPCWGs. We find that the presented structures are simple and easy to fabricate because only one pair of in-axis defects in the PPC tapers is required. The most important result is that we find that the suggested structures can considerably enhance the transmission efficiency for the coupling of light waves between the SWG and PPCWGs. The PPC structure considered here consists of dielectric circular rods of *Si* embedded in a homogenous dielectric medium of *SiO*2 in two-dimensional (2D) triangular lattices. Their refractive indices are 3.45 for *Si* and 1.45 for *SiO*2. The refractive index of the SWG is 1.45 and the SWG is surrounded by air. The band structures of PPC are calculated with the use of plane-wave expansion method.9) We observe that there is one gap for the TM mode with electric fields parallel to the symmetric rod axis, and it is located in the range of $\omega(a/\lambda)$ in [0.26*;* 0.36], with a midgap of $\omega g = 0.30a/\lambda$ when the rod radius is $R = 0.2a$, where a denotes the lattice constant and λ is the wavelength of light in vacuum, $\lambda = 1.55\mu m$, when $a = 0.465\mu m$. The PPCWG is constructed by removing one row of rod array along the W1 direction and its end elements are specially designed by removing five (W5) rods to form a cabin-side-like shape, as shown in the zones marked by the dashed lines in Fig.7.1. This kind of PPCWG is similar to that in refs.[7,8], except for the difference in the tapered structural pattern and the number of defect rod; our design contains only one pair of defect rods.

To achieve the goal of an optimal design for the ending parts of the system to engage in the maximal optical transmission efficiency of the system, it is necessary to search for the ideal patterns at the ending parts of the PPCWGs, which plays a critical role. We intend that the patterns will be simple to allow easy design and fabrication. Therefore, the parameters involved should be as few as possible. We propose a single parameter structure, with only one pair of defect rods separated at two ends of PPCWG, i.e., the entrance and exit terminals of SWG. The tapered structure at the ends consists of 2.5μm-wide/1.5μm -long cabin-side-like PPC taper and then couples light into and out of the finite length of PPCWGs, as shown in Fig. 7.1. Consequently, the optimal design process allows the determination of the optimal positions of this pair of defect rods within the cabin-side-like PPC taper areas, then the mode matching at the interfaces can be achieved with accuracy. The more accuracy the mode matching, the higher the transmission efficiency is. The introduction of this pair of isolated defect rods should result in the significant modification of the modal properties of the guided modes so that mode matching may be markedly improved. The optimal design now becomes simple, because only a single parameter, i.e., the position of defect rods along the *z*-direction, is involved.

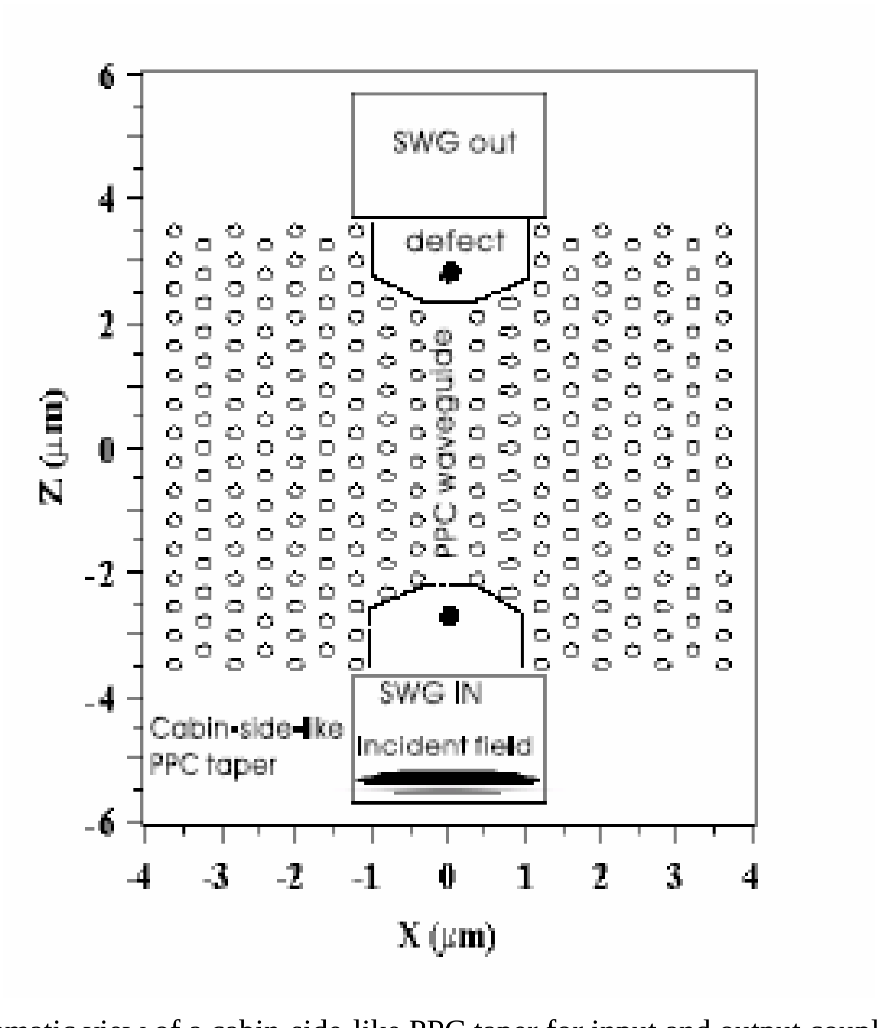

Fig. 7.1 Schematic view of a cabin-side-like PPC taper for input and output couplings.

7.3 Results and discussion

We employ the 2D finite difference time domain (FDTD) method 10) to create a relevant simulation design. A TM polarized Gaussian wave packet centered at λ=1.55μm with the appropriate waveguide mode shape is launched into the system from the entrance of the SWG. Perfectly matched layer(PML) conditions are employed to prevent unwanted reflections.11) The transmitted field is picked up by a power monitor at the output end of the SWG covering the PPCWG exit. The transmission spectrum is calculated from the Fourier-transformed time series and normalized with respect to the launch source. The optimum relative position(z_{opt}) of the defect placed within the cabin-side-like PPC taper was obtained by varying the positionof the defect along the optimized *z*-axis. The transmission of a monochromatic continuous-wave with normalized power is measured at the SWG exit. Therefore, a pair of defects with the same radius as the original rods in the PPCWG are initially employed for scanning the positions that result in the relative maximum transmissions, and at which the defects are set. Regarding the position of the defects along the z-axis(at x=0), the normalized transmitted power obtained as a function of *z* for a given normalized frequency of 0.3(a/λ) is displayed in Fig. 7.2. It can be clearly seen that the maximum of the relative transmission appears at z = 2.75; i.e., at the symmetric coordinates of (0.0,- 2.75) and (0.0,+2.75), the transmission is increased up to 90%. The spectrum shows the coupling efficiency between a fundamental mode of the SWG and a mode of the PPCWG. It should also be noted that the transmission efficiency corresponding to the position of the defect rod at a range of [2.7136, 2.7836]μ*m* along the z-axis is above 80%. This is identically to keep the third rods at (0, 2.78) to count from the input/output end of the PPC tapers along the *W*1-direction. This means that if the transmission demand is only approximately 80%, the additional procedures will be saved by retaining one pair of original rods in the PPC tapers when creating the PPCWG along the *W*1-direction.

A good tapered structure plays a key role in achieving mode matching between the fundamental modes of the wide dielectric SWG and those of the much narrower PPCWG. We calculate the field pattern in the region of the PPC taper and find that the adiabatical reduction of the cross section of the dielectric waveguide occurs in a relatively short distance while still retaining almost perfect throughout. However, the conventional tapered structure in refs.[7, 8] relies upon a greater number of defects and deforms the pattern of defects in order to enhance the transmission efficiency. This is not advantageous for a manufacturing process. One of the reasons is that this type of tapered structure can not support suitable field distributions when using only one pair of defects. Regarding the cabin-side-like taper structures proposed here, the fundamental mode of the SWG is excited by a Gaussian wave that propagates along the *z*-direction (see, Fig. 7.1); thus, the occurrence of resonant peaks in the transmission spectrum of the PPC taper without defects relies upon the distribution of the Bragg reflection along the *W*1¡direction generated by the mode mismatching at the interfaces between the SWG and the PPC taper. Thus, the number of resonant peaks depends strongly on the length of the PPCWG. However, when the cabin-side-like tapers containing a pair of defects placed at the optimal positions are introduced to the system, these peaks in the response are sharply reduced because a more favorable mode matching at the interfaces of the PPCWG is established.

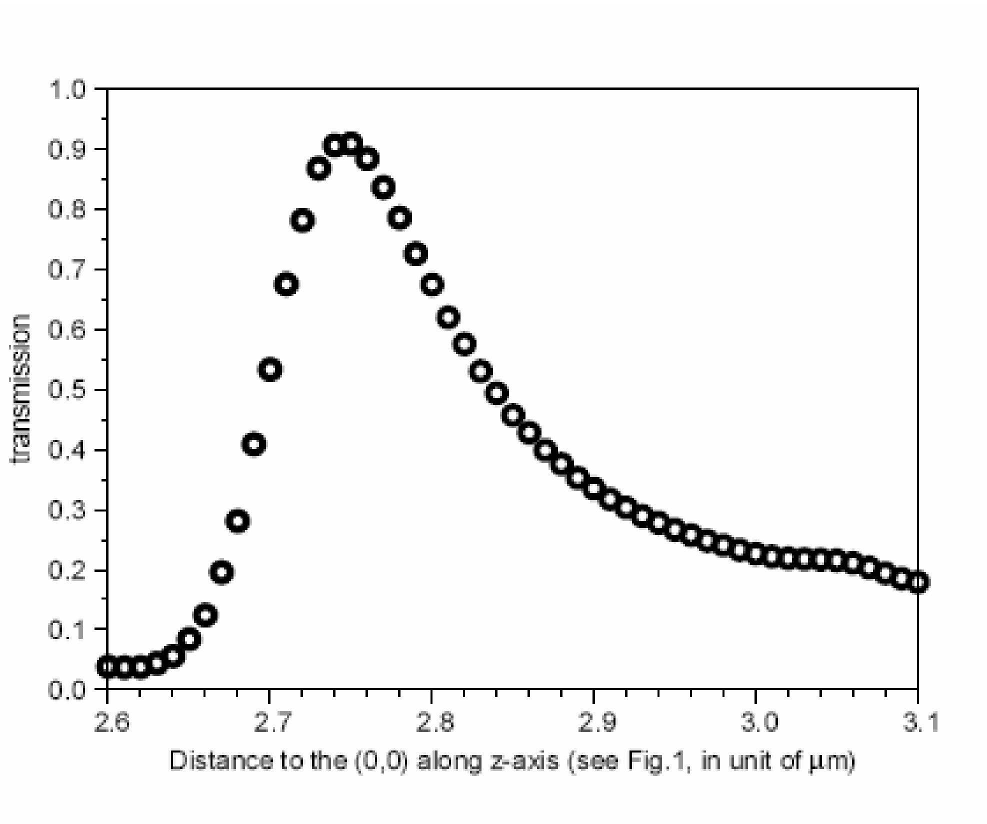

Fig. 7.2 Normalized transmitted power as a function of the *z* coordinate of the isolated defect rods. It is measured at the output-end of the SWG for a given normalized frequency of 0.3(*a*/ λ ¸).

Figures 3(a) and (b) show the steady state of the electric fields (*Ey*) for the input/output coupling when using the cabin-side-like PPC taper in the two cases of (a) without the optimal defect configuration and (b) with it (placed at (0, 2.78)). The wavelength of input light corresponds to λ = *a*/0.3 = 1.55μ*m* and the transmission is 25.45% for Fig. 7.3 (a) and 90.95% for Fig. 7.3 (b). In the simulations, we observe that the shape of the PPC taper structure plays a critical role in changing the coupling efficiency between the conventional SWG and PPC taper, and thus we conclude that the cabin-side-like aspect is superior to the other possible patterns of the PPC taper, particularly for our specified sample, i.e., *Si* dielectric rods embedded in silica medium and set in 2D triangular lattices. The electric field (*Ey*) distributions in the PPCWG with a cabin-side-like structure but without defects are displayed in Fig. 7.3(a), where a standing-wave pattern in the input SWG is apparent. The coupling loss originates from the reflection at the junctions between the SWG and the PPC taper, and therefore, some parts of the field distributions are propagated back into the input end of the SWG, while some decay at the sides of the input-end of SWG. The field distributions exhibit a sinusoidal oscillation inside the PPCWG. When the light waves emerge from the output end of PPC taper, some light waves are propagated inside the output end of the SWG and some decay exponentially in air. It is clearly evident that the field distributions at the output end of the PPC taper, as shown in Fig. 7.3(a), are significantly weaker than those at the input end. Conversely, the field distributions inside the input end of the PPC taper are nearly the same as those at the output end, as evident in Fig. 7.3(b). These results confirm that designing appropriate PPCWG tapered structures containing one pair of defect rods placed at optimal positions can significantly enhance the coupling efficiency and depress the reflection. Therefore, it is expected that the tapered structures provide a favorable environment for establishing suitable field distributions and the introduction of the isolated defect rods can efficiently hold the light waves and form a new diffraction center (the scattering cross section results from a coherent superposition of individual amplitudes of light waves) in the cavity-like structures in the PPC taper region. Consequently, a favorable coupling from the SWG through the PPC taper to the PPC waveguide is achieved when the optimal defect configuration is employed. Note that the constructive interference in the input/output PPC tapers leads to an increase in the coupling efficiency which is mainly attributed to the use of the optimal design defect configuration.

The transmission spectra against the normalized frequency with (circle) and without (square) defects are plotted in Fig. 7.4. An average transmission level of 80% is achieved for a normalized frequency range of [0.295, 0.302]a/λ, indicating that the enhancement of about 50% average transmission level of the sample is achieved with the PPC taper but without the defect rods.

7.4. A brief Comparison Between 2D and 3D Calculation Version

In addition, We have performed the related calculations and we can prove that our tapered structure indeed effectively function with the use of the three-dimensional FDTD method. We find that the obtained results are similar to those presented shown in Fig. 7.3. The study on the coupling effects for our proposed structure in this Letter in the 2D case allows us to qualitatively validate many issues in the design of couplers with a low computational cost, and provides useful information which is directly applicable to the corresponding 3D case. We find that if the size of the sample along the vertical direction, i.e., the y-axis, is sufficiently large (for example, > 10a) the detrimental influence of out-of-plane radiation can be neglected.

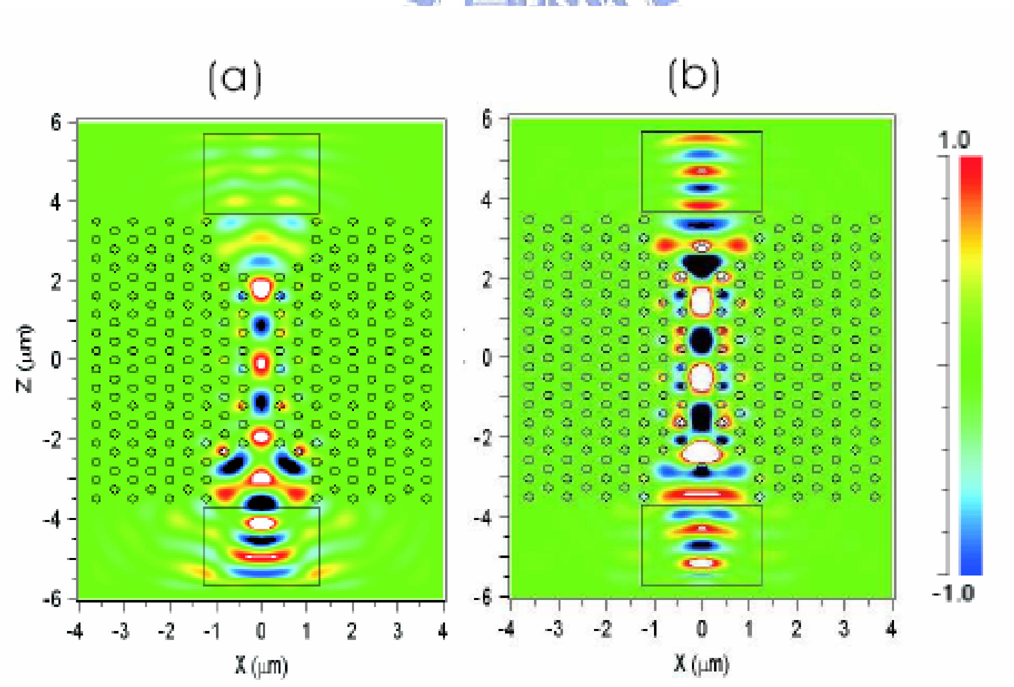

Fig. 7.3 Distributions of the steady electric field intensity when the coupling from the SWG to the PPCWG is adopted with the PPCWG taper shown in Fig.7. 1 for two cases:(a) without the defect rods and (b) with the defect rods placed in the optimal design positions.

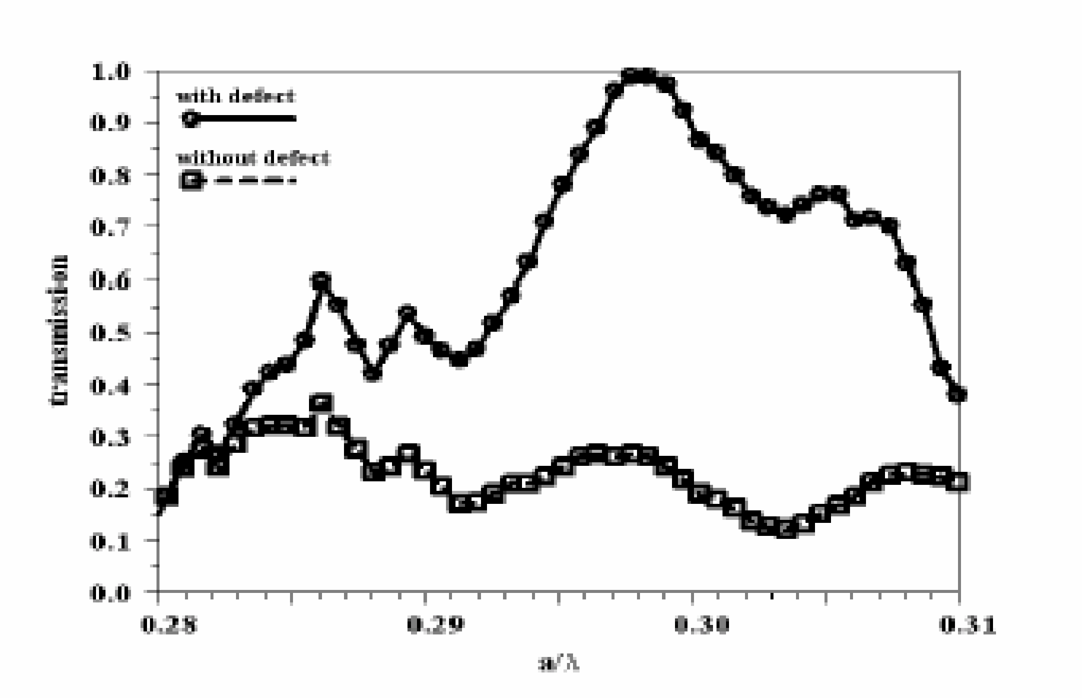

Fig. 7.4 Transmission spectra as a function of normalized frequency for the structures shown in Fig. 7.1 in two cases : (a) without the isolated defect rods at two ends of system (square curve) and (b) with them (circle curve).

7.5 Summary

In conclusion, we have proposed a cabin-side-like PPCWG taper structure containing only a pair of defect rods placed at the two ends of the PPCWG, and calculated the transmission efficiency of the system with the use of the FDTD method. We find that this type of ending structure can substantially improve the mode matching at the interfaces of the junctions, and considerably enhance the coupling efficiency of light waves between the conventional SWG and the PPCWGs. The shape of cabin-side-like structure plays a critical role. The design of the optimal configuration of this type of device can be made by the adjustment of a single parameter, i.e., the varying relative positions of the defect rods along the z-direction; thus, this design procedure becomes simple and easy. The transmitted probability can be increased up to 90% for the optimal designed sample. The another advantage of the presented structures is that the fabrication is easily implemented if the required transmission is only approximately 80%. In addition, the proposed structure is robust against manufacturing inaccuracies and has low costs. It is believed that the proposed structures may be beneficial to various all-optical integrated circuits.

Reference

[1] J. D. Joannopouloulos, P.R. Villeneuve, S.H. Fan, Nature 386(1997)143.

[2] J. D. Joannopouloulos, P.R. Villeneuve, S.H. Fan, Nature 387(1997)830.

[3] Y. Xu, R. Lee, and A. Yariv, Opt. Lett. 25, 755-757 (2000).

[4] A. Mekis and J.D. Joannopoulos, IEEE J. Lightwave Technol. 19, 861-865 (2001).

[5] Ph. Lalanne and A. Talneau, Opt.Express 10, 354 (2002).

[6] A. Talneau, Ph. Lalanne, M. Agio and C.M. Soukoulis, Opt. Lett. 27, 1522-1524 (2002).

[7] P. Sanchis, J. Marti, J. Blasco, A. Martinez and A. Garcia, Opt. Express 10, 1391- 1397 (2002).

[8] Jianhua Jiang, Jingbo Cai, Gregory P. Nordin, and Lixia Li, Opt. Lett. 28, 2381-2383 (2003).

[9] See http://ab-initio.mit.ed/mpb.

[10] A. Taflove, Computational Electrodynamics (Artech, Norwood, MA, 2000).

[11] J. P. Berenger, J. Comput. Phys. 114,185-200 (1994).